

```

EMB-9A 1531: AP--SRGFTFAKHSQTTAVPQCPPGASQLWEGYSLLYVQGNRASGQDLGQPGSCLSKFN 1588
Hs α1(IV) 1440: -PSVDHGFLVTRHSQTIDDPQCPSGTKILYHGYSLLYVQGNtk75ERAHGQDLGTAGSCLRKFS 1498

EMB-9A 1589: TMPFMFCNMNSVCHVSSRNDYSFWLSTDEPMTPMNPNVTGTAIRPYISRCVCEVPTQII 1648
Hs α1(IV) 1499: TMPFLEFCNINNVCFASRNDYSYWLSTPEPMPMSMAFITGENIRPFISRCVCEAFAMVM 1558

EMB-9A 1649: AVHSQDTSVPQCPCQGWSGMWTGYSFVMHTAAGAEGTGQSLQSPGSCLEEFRAVVFIECHG 1708
Hs α1(IV) 1559: AVHSQTIQIPPCPSGWSSIWIGYSFVMHTSAGAEGSGQALASPGSCLEEFRSAPFIECHG 1618

EMB-9A 1709: RGTCNYYATNHGFWLSIVDQDKQFRKPMSTLKGGLKDRVSRQVCLKNR 1759
Hs α1(IV) 1619: RGTCNYYANAYSFWLATIERSEMFKKPTPSTLKAGELRTHVSRQVCMRRT 1669

```

**Figure S1** EMB-9(*tk75*) has a substitution at an evolutionarily conserved amino acid in the NC1 domain. Alignment of the C-terminal NC1 domain sequences of the type IV collagen  $\alpha 1$  chains of *C. elegans* (EMB-9) and humans [Hs  $\alpha 1$  (IV)]. The amino acids in the trimer-trimer interface region (Sundaramoorthy *et al.* 2002) are underlined in magenta. Identical amino acids are boxed (black). The mutated glycine in *tk75* is indicated.

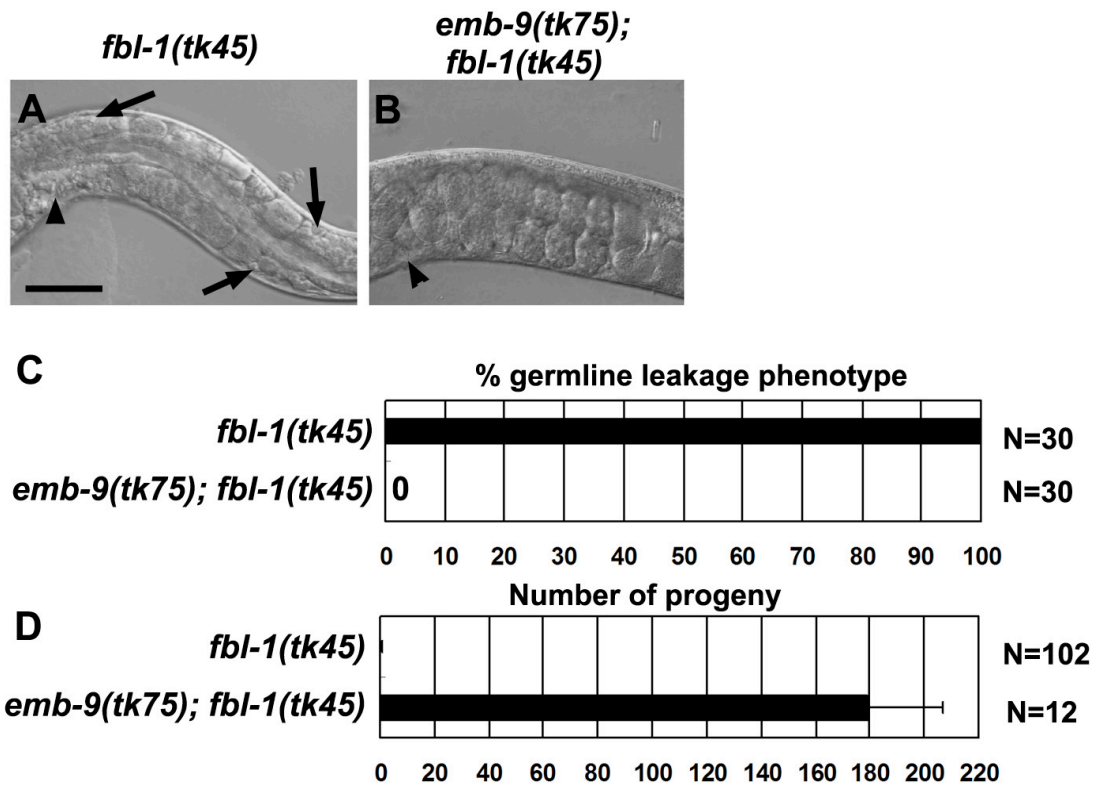


**Figure S2** Germ line phenotype. (A) The germ cells (arrows) were released into the body cavity in 1-day-old *fbl-1(tk45)* adult hermaphrodites, probably because of the defects in the BM. (B) This phenotype was not observed in 1-day-old *emb-9(tk75); fbl-1(tk45)* adult hermaphrodites. Arrowheads point to the vulvae. Scale bar, 25  $\mu$ m. Quantification of the germ line phenotype (C), n = 30. One-day-old adult hermaphrodites were scored for the presence of germ cells in the body cavity by Nomarski microscopy; Quantification of brood sizes (D), n = 102 for *fbl-1(tk45)* and n = 12 for *emb-9(tk75); fbl-1(tk45)*. Brood size is the number of hatched larvae from eggs laid by an adult hermaphrodite during 72 hours.

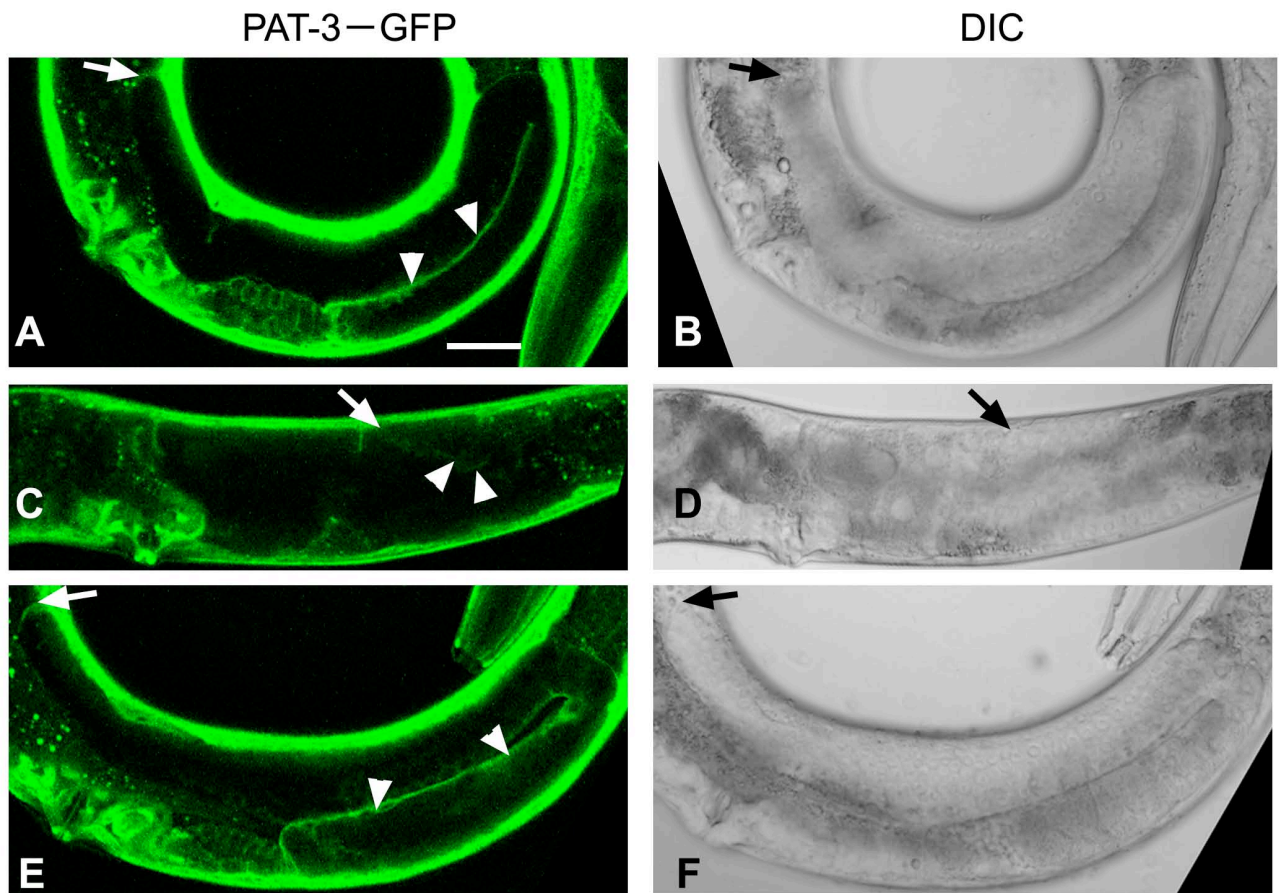


**Figure S3** PAT-3-GFP expression in the gonadal sheath cells. Confocal (A, C, E) and Nomarski (B, D, F) images of posterior gonads of wild-type (A, B), *fbl-1(tk45)* (C, D), and *emb-9(tk75); fbl-1(tk45)* (E, F) young adult hermaphrodites expressing PAT-3-GFP. Arrows indicate PAT-3-GFP expression in DTCs. Arrowheads indicate PAT-3-GFP expression in gonadal sheath cells. The weakened PAT-3-GFP expression in DTCs and sheath cells in *fbl-1(tk45)* animals (C, D) recovered to wild-type levels in *emb-9(tk75); fbl-1(tk45)* animals (E, F). All images were captured under the same conditions. Scale bar, 25  $\mu$ m.

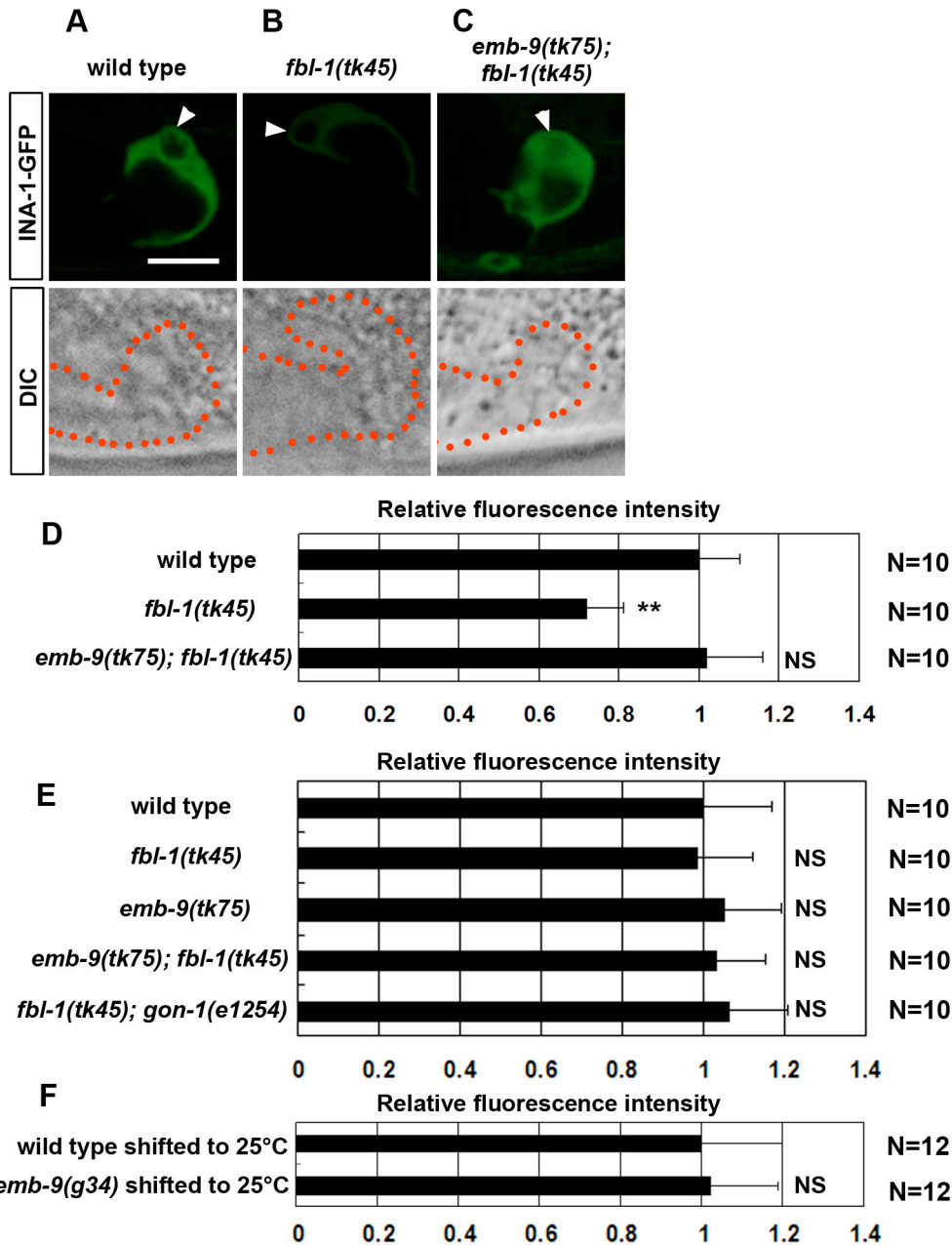


**Figure S4** INA-1-GFP expression in DTCs. Images were captured by CSU-X1 spinning-disc confocal system (Yokogawa Electric Corp.) mounted on Axioplan 2 microscope (Zeiss) equipped with a C-apochromat 63X (water immersion; NA 1.2) lens and controlled by MetaMorph software (Molecular Devices Inc.). (A, B, C) *ina-1::GFP* expression. Confocal (upper) and Nomarski (lower) images of L3 hermaphrodites of wild type (A), *fbl-1(tk45)* (B), *emb-9(tk75); fbl-1(tk45)* (C) having *gmls5* that contain chromosomally integrated *ina-1::GFP* plasmids (Baum & Garriga 1997). The arrowhead indicates the INA-1-GFP expression in DTCs. Scale bar, 20  $\mu$ m. (D) Fluorescence intensity of INA-1-GFP. The fluorescence intensity for each sample was normalized to that of the wild type. Ten confocal

images of DTCs for each strain were used for quantification. The relative fluorescence intensity was determined as in Figure 5G. Data are shown as the mean  $\pm$  SD. Results for Student's *t*-test versus wild type are indicated; \*\*,  $P < 0.01$ ; NS, not significant. All images were captured under the same conditions. (E, F) *lag-2p::GFP* expression. As a control, we examined *lag-2p::GFP* expression in DTCs and found that it is not affected by genetic backgrounds used in this work. All strains have *q/s56* that contains chromosomally integrated *lag-2p::GFP* plasmids (Blelloch *et al.* 1999) in their background. The fluorescence intensity for each sample was normalized to that of the wild type. Ten or twelve confocal images of DTCs for each strain were used for quantification. The relative fluorescence intensity was determined as in Figure 5G. Data are shown as the mean  $\pm$  SD. Results for the Student's *t*-test against the wild-type value are indicated; NS, not significant. All images were captured under the same conditions.

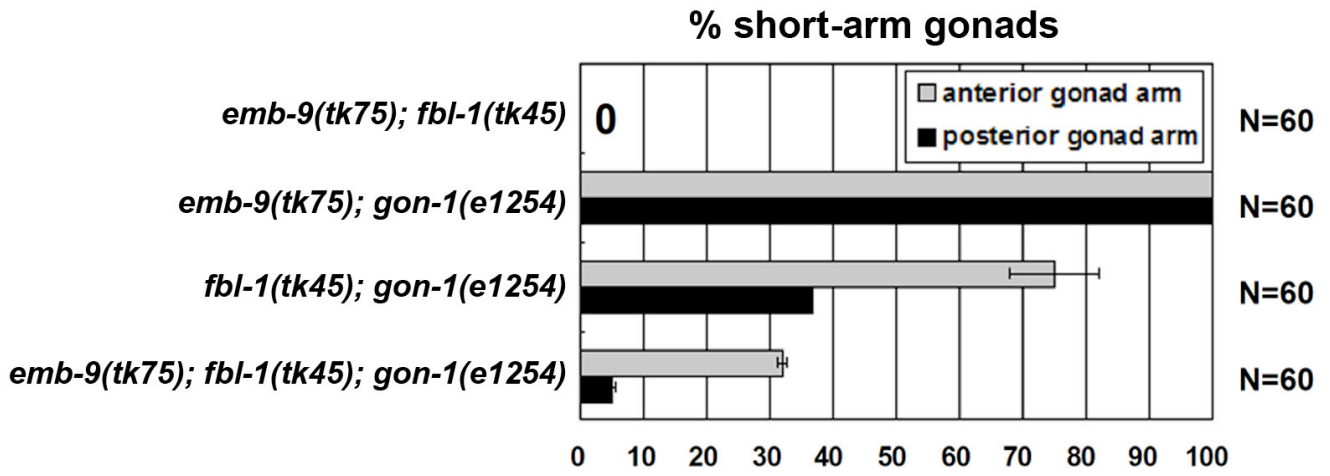


**Figure S5** Gonadal elongation defects in the *emb-9(tk75); fbl-1(tk45); gon-1(e1254)* triple mutants  
 Data for double mutants are included for comparison.

## LITERATURE CITED

- Baum, P. D., and G. Garriga, 1997 Neuronal migrations and axon fasciculation are disrupted in *ina-1* integrin mutants. *Neuron* **19**: 51-62.
- Blelloch, R., S. S. Anna-Arriola, D. Gao, Y. Li, J. Hodgkin *et al.* 1999 The *gon-1* gene is required for gonadal morphogenesis in *Caenorhabditis elegans*. *Dev.Biol.* **216**: 382-393.
- Sundaramoorthy, M., M. Meiyappan, P. Todd, and B. G. Hudson, 2002 Crystal structure of NC1 domains. Structural basis for type IV collagen assembly in basement membranes. *J.Biol.Chem.* **277**: 31142-31153.